

Computational Analysis of *Plasmodium falciparum* RNA-Seq data reveals PPIs that might be implicated in the Invasion of the RBCs

Jumoke Soyemi
dept. of Computer Science
Federal Polytechnic
Ilaro, Nigeria
jumoke.soyemi@federalpolyilaro.edu.ng

Rotimi Solomon
dept. of Biological Sciences
Covenant University
Ota, Nigeria
ola.rotimi@covenantuniversity.edu.ng

Itunuolwa Isewon
dept. of Computer & Inform. Sciences
Covenant University
Ota, Nigeria
itunu.isewon@covenantuniversity.edu.ng

Jelili Oyelade
dept. of Computer & Inform. Sciences
Covenant University
Ota, Nigeria
ola.oyelade@covenantuniversity.edu.ng

Olubanke Ogunlana
dept. of Biological Sciences
Covenant University
Ota, Nigeria
banke.ogunlana@covenantuniversity.edu.ng

Ezekiel Adebiyi
dept. of Computer & Inform. Sciences
Covenant University
Ota, Nigeria
ezekiel.adebiyi@covenantuniversity.edu.ng

Abstract—In this study, differentially expressed genes for the trophozoite and schizont stages of *Plasmodium falciparum*'s life cycle were extracted from a time series RNA-Seq gene expression experiment. About 28% of the 5,270 genes used in the experiment were found to show significant expression at these stages. Enrichment analysis using Gene Ontology implicated a total of 62 functions as highly enriched from the list of differentially expressed genes (DEGs). Some include; protein targeting to membrane, protein import, establishment of proteins localization to organelle, ribonucleic protein complex, nucleotide-excision repair and processes related to the mitochondria. A protein interaction network (PIN) for the DEGs at the schizont stage was extracted from experimental data of protein-protein interactions and supplemented with data from a protein interaction database. We predicted a number of protein-protein interactions in *Plasmodium falciparum* that may be implicated in invasion of the human red blood cells (RBCs). Some of these predictions are consistent with those from previous studies while quite a number of them are novel. We also identified 16 protein complexes from the PIN using the Molecular Complex Detection (MCODE) algorithm. The functional enrichment of the identified protein complexes showed functions related to gene expression, translation, RNA transport and metabolic/biological processes which have been identified to be important in the invasion process. The result from this study is meant to provide better insight into disease at hand.

Keywords— RNA-Seq gene expression data, *Plasmodium falciparum*, Gene Ontology, MCODE Algorithm, Differentially Expressed genes

I. INTRODUCTION

The invasion of the erythrocytes is critical to the survival and pathogenesis of the popular malaria parasite, *Plasmodium falciparum* (P.f.). The preliminary interaction between the merozoite and the red blood cell is a vital key since the parasite must separate between erythrocytes competent for invasion and other cell types [1, 2]. Therefore, a tight junction must be

established between the parasite and the host red cell membrane before the parasite can gain entrance into the red blood cells. This tight junction moves from the apical to the posterior end of the merozoite in a complex turn of activities powered by the parasite actin-myosin motor [3, 4]. A structure called the parasitophorous vacuole is created when the parasite makes its way into the host cell and encloses itself against the cytoplasm of the host cell to create a hospitable environment for its development. Invasion by the parasite thus causes vast changes in the host RBCs particularly, the increase in the rigidity of the membrane which assists the parasite to survive within the cell of its host contributing to an increase in disease malignity [5]

The process of invasion involves specific proteins whose majority interacts with other proteins to form protein interaction networks (PIN). Protein-protein interactions (PPIs) are vital key processes activating various biological events. Invasion of the RBCs by *Plasmodium falciparum*'s merozoite has been projected as a possible target for antimalarial drugs [6, 7, 8]. Presently there are no current antimalarial drugs against host cell invasion [9]; hence, there is a renewed research effort towards obtaining drug targets at this level. The inhibition of merozoite from invading the RBCs, would lead to instant disruptions of the parasite's lifecycle [10, 11, 12]. Also, study [13] presented a review of the potentials of the merozoite surface protein (MSP) as a possible malaria vaccine. The aim of this study therefore is to predict the protein-protein interactions of the *Plasmodium falciparum*'s schizont stage responsible for host cell invasion using RNA-seq gene expression data. The findings should provide more insight in discovering drug targets that could be used in blocking merozoite invasion of the RBCs.

II. MATERIALS AND METHODS

A. Time-Course Data

RNA-Seq gene expression data for P.f. was obtained from Otto *et al.* [14]. The study used RNA-sequencing to capture the entire asexual intra-erythrocytic developmental cycle of P.f. from the ring stage to mature schizonts over seven time points. The data contains 5270 normalized gene expression values. Time courses for trophozoite and schizont stages were extracted from the data at four-time points (24h, 32h, 40h and 48h) and analyzed for differential expression.

B. Differentially Expressed Genes

To discover the differentially expressed genes at the schizont stage, an R package called maSigPro [15] was used. Although, maSigPro was originally designed for microarray data, it has now been updated to handle RNA-seq data. It works by finding genes with differential temporal expression changes using a two-step regression approach. This step-wise regression analysis was carried out to discover differentially expressed profiles. The cut-off value for the R-squared of the regression value was set at 0.7.

C. Functional Enrichment

We performed gene functional enrichment analysis for the differentially expressed genes on PlasmoDB¹. The biological processes with top ranked gene ontology (GO) terms were reported. P-value cut off was set at 0.05.

D. Protein Interaction Data

Protein-protein interaction data for P.f. was obtained from [16]. *Plasmodium falciparum* of PPIs were identified using high-throughput yeast two-hybrid (Y2H) experiment which bypasses the complexities experienced in expressing P.f. proteins. The study identified 2,846 unique interactions from more than 32,000 Y2H screens with P.f. protein fragments [16]. The Search Tool for Retrieval of Interacting Gene/Proteins (STRING) database² contains 30,015 PPI. From [16] dataset, protein interaction data was extracted for proteins that are synthesized by our DEGs. This was supplemented by PPIs from STRING database.

E. Protein Complex Detection and Enrichment Map (EM)

Analysis of the network for clusters of the protein interaction network (PIN) using the Molecular Complex Detection (MCODE) algorithm was performed in Cytoscape (version 3.4.0)³. Node score cut-off was set at 0.2, false degree cut-off was set at 2, K-core was set at 2 and maximum depth from seed was set at 100. The enrichment map analysis was done using Enrichment map⁴ (EM) plugin in Cytoscape. Both

the expression data and enrichment result were supplied to EM. The P-value cut-off was set at 0.05, false discovery rate (FDR) Q-value cut-off at 0.1 and overlap coefficient cut-off at 0.5, after which the map was built. Functional enrichment of our protein complexes was done using DAVID⁵ functional classification tool.

III. RESULTS

The gene expression data was investigated for differential expression using Regression analysis. Figure 1 is a plot of the resulting 1,538 differentially expressed gene profiles found at the trophozoite and schizont stages from our analysis. The expression profile plot shows increased activities of the DEGs between (24h to 32h) and (40h to 48h), this tends to decrease continuously between 32h to 40h. The details of the DEGs are presented in supplementary file S01. The X axis with label x24h and x32h represent the time points of early and late trophozoite stage while the x40h and x48h represent the time points of schizont early and late stages.

A. Gene Ontology Functional Enrichment

The gene ontology functional enrichment of the DEGs is presented in table 1 and sorted according to their p-values. The first 9 functions are highly-expressed and they include gene expression, translation, cellular process, macromolecule metabolic process and others. Eighteen (18) functions have percentage of background genes count in the result greater than or equal to 60%, these have been highlighted in blue. The metabolic pathway enrichment revealed 19 pathways that are enriched as presented in Table 2. Aminoacyl-tRNA biosynthesis pathway shows a significant p-value of 4.96970407014E-1. Three pathways showed significant enriched functions: Aminoacyl-tRNA biosynthesis, Drug metabolism-other enzymes and Phenylalanine metabolism.

B. Protein Interaction Network

A total of 516 PPIs were reported from the PPI data by [16] for our DEGs. From STRING database, a total of 1041 PPI were extracted after a threshold of 0.95 was set as cut-off. The two datasets were combined resulting in a PIN with 1,538 PPIs (see supplementary file S02).

C. Protein Complex Detection and Enrichment Map Analysis

MCODE algorithm in CYTOSCAPE was used to predict protein complexes of our PIN. The MCODE algorithm detected a total of the sixteen complexes. We have displayed the first four clusters in this paper in figure 2. Cluster 1 has 54 nodes, 713 edges and a density score of 26.868. Cluster 2 has 9 nodes, 35 edges and a score of 8.75. Cluster 3 has 7 nodes, 21 edges with a score of 7 and Cluster 4 has 5 nodes, 10 edges and a

¹ www.plasmodb.org

² <https://string-db.org>

³ <http://www.cytoscape.org>

⁴ www.balerlab.org/Software/EnrichmentMap

⁵ <https://david.ncifcrf.gov>

density score of 5. The other complexes are sparsely clustered presents an enrichment map of the enriched GO terms for the PPIs.

D. Detected Protein Complexes and their Functions

We performed the functional enrichment of each of the sixteen protein complexes with detailed description of the functions of the first seven clusters presented in table 3. Cluster 1 consists of 54 proteins associated with translation, ribosome, ribonucleoprotein and structural constituents of the ribosome. Cluster 2 has 9 proteins implicated in formation of translation preinitiation complex, RNA transport, regulation of translational initiation and protein biosynthesis. There are 7. proteins in Cluster 3 involved in endopeptidase activity, proteasome core complex, ubiquitin-dependent protein

in the number of resulting nodes, edges and scores Figure 3 catabolic process, nucleus and threonine-type endopeptidase activity. Cluster 4 consists of 5 proteins having the following functions; nuclear polyadenylation-dependent tRNA catabolic process, nuclear exosome (RNase complex), nuclear polyadenylation-dependent tRNA catabolic process and RNA degradation. Supplementary file S03 presents a table of the sixteen protein complexes that are active during RBC invasion by the merozoites with the actual proteins interacting together to make this actions possible and the functions enriched.

E. Important PPIs Identified

Based on the important proteins identified in study [17], we were able to predict key protein-protein interactions of these proteins and we have reported these in table 4.

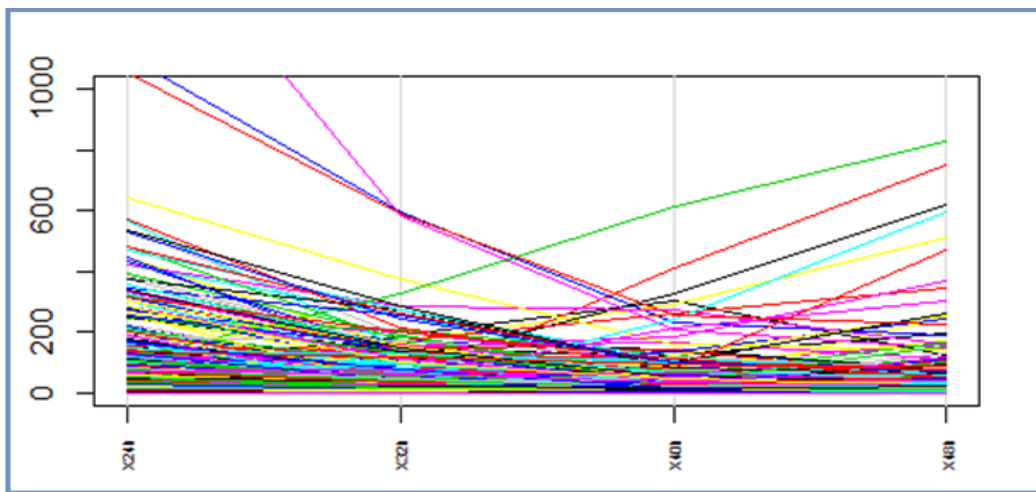


Fig.1. Expression Profiles of the Differentially Expressed Genes at the schizont stage

TABLE I. Gene Ontology Functional Enrichment

ID	Name	Bgd Counts	Result Counts	Percentage of Bgd	Fold Enrichment	P-value
GO:0010467	gene expression	615	257	41.8	1.45	8.17E-08
GO:0006412	Translation	313	147	47	1.63	5.51E-07
GO:0043170	macromolecule metabolic process	1263	446	35.3	1.22	1.03E-05
GO:0044260	cellular macromolecule metabolic process	1176	416	35.4	1.22	2.19E-05
GO:0009987	cellular process	1961	646	32.9	1.14	6.10E-05
GO:0044238	primary metabolic process	1510	512	33.9	1.17	6.82E-05
GO:0044237	cellular metabolic process	1484	504	34	1.18	7.11E-05
GO:0019538	protein metabolic process	795	291	36.6	1.27	9.23E-05
GO:0034645	cellular macromolecule biosynthetic process	507	198	39.1	1.35	9.87E-05
GO:0008152	metabolic process	1675	559	33.4	1.16	0.00010528
GO:0009059	macromolecule biosynthetic process	508	198	39	1.35	0.00010801
GO:0016070	RNA metabolic process	380	155	40.8	1.41	0.00012191
GO:0044267	cellular protein metabolic process	706	260	36.8	1.28	0.00017729
GO:0044249	cellular biosynthetic process	666	244	36.6	1.27	0.00038045

GO:0009058	biosynthetic process	678	247	36.4	1.26	0.00045776
GO:0006520	cellular amino acid metabolic process	87	47	54	1.87	0.00049194
GO:0043038	amino acid activation	48	29	60.4	2.09	0.00166358
GO:0043039	tRNA aminoacylation	48	29	60.4	2.09	0.00166358
GO:0006418	tRNA aminoacylation for protein translation	48	29	60.4	2.09	0.00166358
GO:0008150	biological_process	2643	820	31	1.07	0.00290179
GO:0006082	organic acid metabolic process	139	62	44.6	1.54	0.00302376
GO:0043436	oxoacid metabolic process	139	62	44.6	1.54	0.00302376
GO:0019752	carboxylic acid metabolic process	139	62	44.6	1.54	0.00302376
GO:0090304	nucleic acid metabolic process	527	190	36.1	1.25	0.00332838
GO:0017038	protein import	26	18	69.2	2.4	0.00443886
GO:0042180	cellular ketone metabolic process	145	63	43.4	1.5	0.00448746
GO:0072594	establishment of protein localization to organelle	22	16	72.7	2.52	0.00512165
GO:0006605	protein targeting	36	22	61.1	2.12	0.00525658
GO:0033365	protein localization to organelle	35	21	60	2.08	0.00735272
GO:0008380	RNA splicing	61	31	50.8	1.76	0.00825487
GO:0006839	mitochondrial transport	17	13	76.5	2.65	0.00847362
GO:0007005	mitochondrion organization	15	12	80	2.77	0.00891084
GO:0072655	establishment of protein localization in mitochondrion	13	11	84.6	2.93	0.00923888
GO:0006626	protein targeting to mitochondrion	13	11	84.6	2.93	0.00923888
GO:0070585	protein localization in mitochondrion	13	11	84.6	2.93	0.00923888
GO:0006807	nitrogen compound metabolic process	674	230	34.1	1.18	0.01045941
GO:0034641	cellular nitrogen compound metabolic process	669	228	34.1	1.18	0.01130518
GO:0034660	ncRNA metabolic process	130	55	42.3	1.46	0.01138199
GO:0032268	regulation of cellular protein metabolic process	28	17	60.7	2.1	0.01395186
GO:0000375	RNA splicing, via transesterification reactions	44	23	52.3	1.81	0.01678256
GO:0006139	nucleobase-containing compound metabolic process	630	213	33.8	1.17	0.0185421
GO:0006417	regulation of translation	22	14	63.6	2.2	0.0188197
GO:0010608	posttranscriptional regulation of gene expression	25	15	60	2.08	0.02178651
GO:0031323	regulation of cellular metabolic process	172	67	39	1.35	0.02214412
GO:0016071	mRNA metabolic process	79	35	44.3	1.53	0.02395823
GO:0006399	tRNA metabolic process	84	36	42.9	1.48	0.03140364
GO:0006396	RNA processing	195	73	37.4	1.3	0.03307346
GO:0051246	regulation of protein metabolic process	32	17	53.1	1.84	0.03318666
GO:0080090	regulation of primary metabolic process	174	66	37.9	1.31	0.03417276
GO:0010468	regulation of gene expression	148	57	38.5	1.33	0.03825995
GO:0009889	regulation of biosynthetic process	142	55	38.7	1.34	0.03839514
GO:0031326	regulation of cellular biosynthetic process	142	55	38.7	1.34	0.03839514
GO:0006457	protein folding	83	35	42.2	1.46	0.03926259
GO:0019222	regulation of metabolic process	185	69	37.3	1.29	0.03956321
GO:0006612	protein targeting to membrane	13	9	69.2	2.4	0.03987776
GO:0006397	mRNA processing	75	32	42.7	1.48	0.04244287
GO:0000398	nuclear mRNA splicing, via spliceosome	36	18	50	1.73	0.04271194

GO:0000377	RNA splicing, via transesterification reactions with bulged adenosine as nucleophile	36	18	50	1.73	0.04271194
GO:0006289	nucleotide-excision repair	11	8	72.7	2.52	0.04353138
GO:0010556	regulation of macromolecule biosynthetic process	141	54	38.3	1.33	0.04590157
GO:2000112	regulation of cellular macromolecule biosynthetic process	141	54	38.3	1.33	0.04590157
GO:0022618	ribonucleoprotein complex assembly	16	10	62.5	2.16	0.04750479

TABLE II. Metabolic Pathway Enrichment

ID	Name	Bgd count	Result count	percentage of bgd	Fold enrichment	P-value
ec00970	Aminoacyl-tRNA biosynthesis	45	30	66.7	5.14	4.97E-11
ec00230	Purine metabolism	98	28	28.6	2.2	0.000226217
ec00240	Pyrimidine metabolism	81	23	28.4	2.19	0.000944635
ec00010	Glycolysis / Gluconeogenesis	26	11	42.3	3.26	0.00194336
ec00330	Arginine and proline metabolism	15	8	53.3	4.11	0.002750455
ec00270	Cysteine and methionine metabolism	12	7	58.3	4.5	0.00352225
ec00480	Glutathione metabolism	28	10	35.7	2.75	0.008161837
ec00983	Drug metabolism - other enzymes	8	5	62.5	4.82	0.01120959
ec00620	Pyruvate metabolism	25	9	36	2.78	0.011489275
ec00860	Porphyrin and chlorophyll metabolism	12	6	50	3.86	0.01194293
ec00710	Carbon fixation in photosynthetic organisms	13	6	46.2	3.56	0.015829397
ec00250	Alanine, aspartate and glutamate metabolism	13	6	46.2	3.56	0.015829397
ec00680	Methane metabolism	10	5	50	3.86	0.021608394
ec00071	Fatty acid degradation	20	7	35	2.7	0.0280162
ec00260	Glycine, serine and threonine metabolism	11	5	45.5	3.51	0.028580995
ec00360	Phenylalanine metabolism	4	3	75	5.78	0.036684632
ec00052	Methane metabolism	8	4	50	3.86	0.039599312
ec00520	Amino sugar and nucleotide sugar metabolism	17	6	35.3	2.72	0.039930781

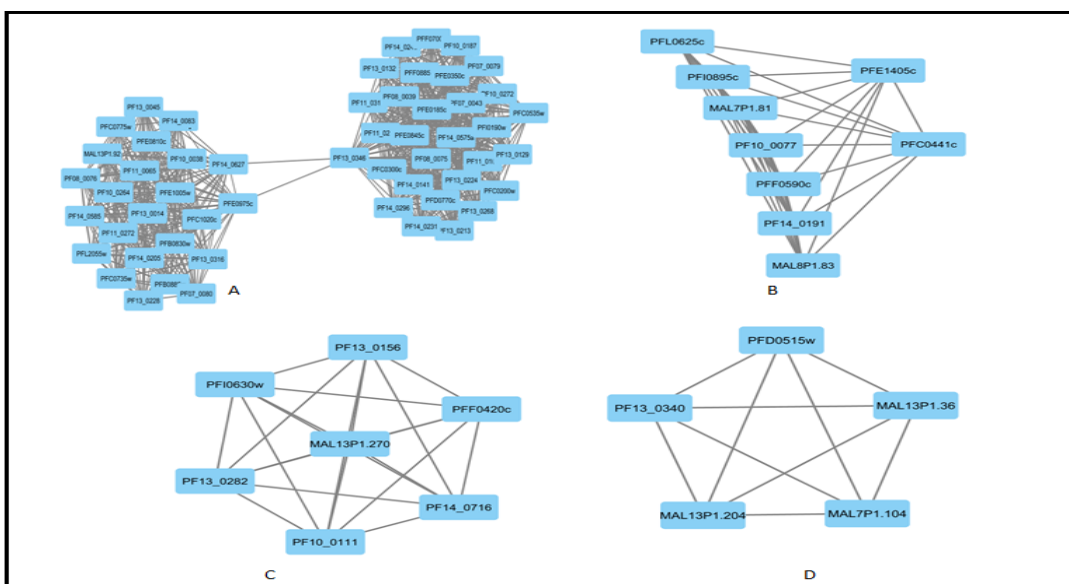


Fig. 2. Predicted protein complexes (A-D) for clusters 1-4 respectively

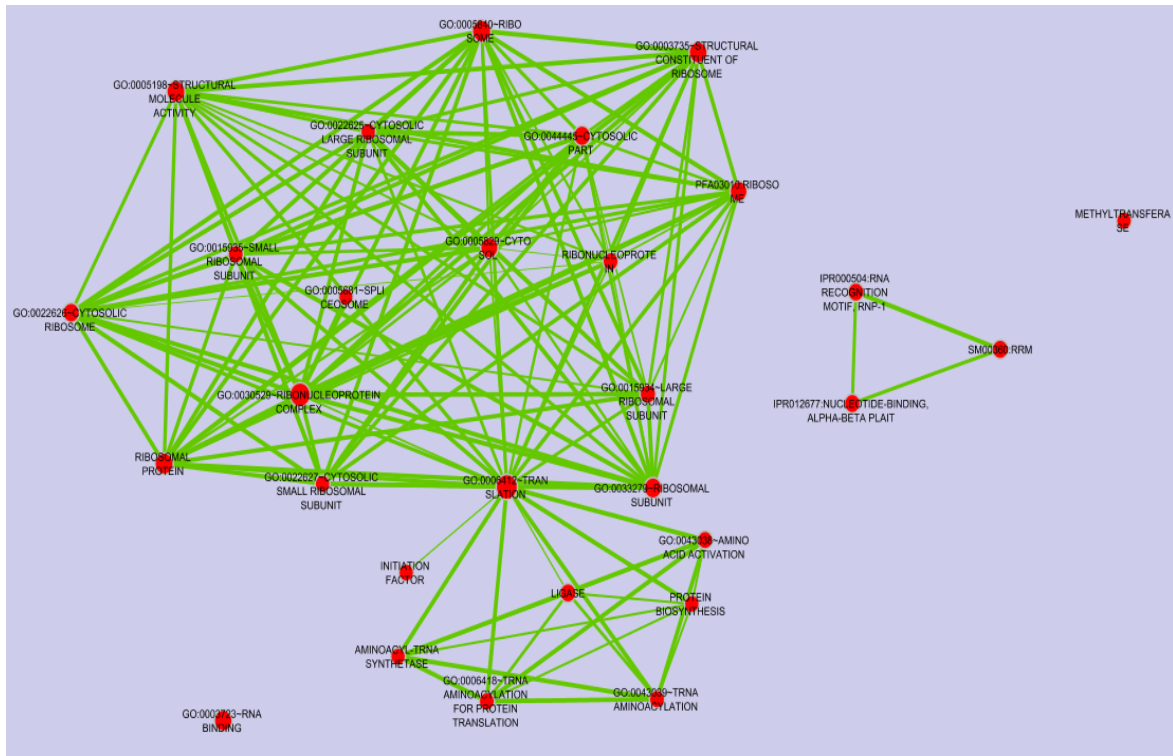


Fig. 3. Enrichment Map

TABLE III. Protein complexes and their functions

Clusters	Functions Enriched	Enriched Scores	Count	P_value
Cluster 1 Nodes: 54 Edges: 713 Score: 26.868	Ribosomal Protein Ribonucleoprotein Structural constituent of ribosome translation Ribosome	64.58	49	3.8E-79
Cluster 2 Nodes: 9 Edges: 35 Score: 8.75	eukaryotic translation initiation factor 3 complex eukaryotic 43S preinitiation complex eukaryotic 48S preinitiation complex Initiation factor formation of translation preinitiation complex regulation of translational initiation translation initiation factor activity Cytoplasm Protein biosynthesis RNA transport	12.67	7 7 7 8 7 7 7 8 8 8	8.3E-16 1.8E-15 1.8E-15 1.3E-14 3.2E-14 1.7E-13 3.4E-13 6.6E-13 1.7E-12 3.0E-6
Cluster 3 Nodes: 7 Edges: 21 Score: 7	Proteasome proteasome core complex Proteasome, subunit alpha/beta threonine-type endopeptidase activity endopeptidase activity Proteasome Nucleus ubiquitin-dependent protein catabolic process Hydrolase Nucleus	9.21	7 6 6 6 6 7 6 6 6 6	1.8E-14 3.7E-12 3.9E-12 4.4E-12 9.7E-11 4.1E-10 8.0E-9 2.4E-8 2.3E-5 4.1E-5
Cluster 4 Nodes: 5 Edges: 10 Score: 5	nuclear exosome (RNase complex) exonucleolytic trimming to generate mature 3'-end of 5.8S rRNA from tricistronic rRNA transcript (SSU-rRNA, 5.8S rRNA, LSU-rRNA) exonucleolytic nuclear-transcribed mRNA catabolic process involved in deadenylation-dependent decay nuclear polyadenylation-dependent rRNA catabolic process nuclear polyadenylation-dependent tRNA catabolic process	7.16	5 4 4 4 4	2.6E-11 7.9E-9 7.9E-9 7.9E-9 9.6E-8

Cluster 5 Nodes: 5 Edges: 10 Scores: 5	3'-5'-exoribonuclease activity -RNA degradation Phagosome ATP hydrolysis coupled proton transport proton-transporting ATPase activity, rotational mechanism Oxidative phosphorylation Metabolic pathways Hydrolase	4.8	5 4 4 5 5 3	2.3E-7 7.2E-7 7.8E-7 1.0E-6 3.3E-3 3.8E-2
Cluster 6 Nodes: 5 Edges: 9 Score: 4.5	DNA-directed RNA polymerase transcription from RNA polymerase II promoter DNA-directed RNA polymerase activity RNA polymerase Nucleotidyltransferase	4.28	4 4 4 4 3	5.7E-7 9.0E-7 5.6E-6 8.7E-6 5.6E-4
Cluster 7 Nodes: 9 Edges: 17 Score: 4.25	RNA degradation U6 snRNP U4/U6 x U5 tri-snRNP complex	5.07	5 3 3	5.1E-5 7.7E-5 6.9E-4

TABLE IV. Important Protein-Protein Interactions Predicted from our study

Group Name	Name	Important Merozoite Proteins identified	Protein-protein interaction
Surface Proteins	MSP-1	PFI1475w	PFI1475w- PFE0595w
	MSP-2	PFB0300c	PFB0300c- PFL1530w
	MSP-2	PFB0300c	PFB0300c- PF13_0129
	Pf38	PFE0395c	PFE0395c-PF13_0058
Microneme Proteins	EBA-140/BAEBL	MAL13P1.60	MAL13P1.60-PFC0265c
	ASP	PFD0295c	PFD0295c-PFL1330c
Peripheral Surface Proteins	ABRA	PFL1385c	PFL1385c-PFI0370c
	MSP3	PF10_0345	PF10_0345-PFC0805w
Rhoptry Neck Proteins	GLURP	PF10_0344	PF10_0344-PFB0125c
	SERA4	PFB0345c	PFB0345c-MAL7P1.7
	SERA5	PFB0340c	PF10_0136-PFB0340c
	SERA5	PFB0340c	PFB0340c-chr13_2000027.gen_4
		PFB0340c	PFB0340c-PFE0285c
	SERA6	PFB0335c	PF11_0200-PFB0335c
	Rh2a	PF13_0198	PF13_0198-PF10_0294
	Rh2b	MAL13P1.176	PFI1650w-MAL13P1.176

IV. DISCUSSION

This study predicted 1510 DEGs from our study with important functions enriched. Sixteen protein complexes that might be implicated in the invasion process were also predicted together with their enriched functions. Our study was able to predict the protein-protein interactions of some notable proteins that help in the invasion process (table 4). We have presented the key protein-protein interactions out of the 1538 PPIs predicted in our study to be implicated in invasion process in table 4. Several of the other PPIs predicted are consistent with predictions from literature.

We captured four key PPIs that are active as MSP (PFI1475w-PFE0595w, PFB0300c-PFL1530w, PFB0300c-PF13_0129 and PFE0395c-F13_0058). Merozoite surface

proteins are used as either integral membrane proteins, glycolphosphatidylinositol (GPI)-anchored proteins or peripherally-associated proteins. These proteins are expressed on the surface of the merozoite prior to invasion by a variety of mechanisms and are therefore important for the invasion process.

Two key PPIs as Microneme proteins were identified (MAL13P1.60-PFC0265c and PFD0295c-PFL1330c). Microneme proteins play important role in the recognition, adhesion and invasion of host cells (table 4).

The key PPIs of peripheral surface proteins identified in this study are PFL1385c-PFI0370c, PF10_0345-PFC0805w, PF10_0344-PFB0125c, PFB0345c- MAL7P1.7, PF10_0136-PFB0340c, PFB0340c-chr13_2000027.gen_4, PFB0340c-PFE0285c, and PF11_0200-PFB0335c. Preipheral surface

proteins are candidates for binding to erythrocyte receptors as they binds to the surface of developing merozoites and are directly involved in invasion (table 4).

Some of the important PPIs of Rhopty neck proteins discovered in our study are PF13_0198-PF10_0294 and PF1650w-MAL13P1.176. In the invasion process, apicomplexan parasites form a close tight junction form active gliding with the host cell and this tight junction is the one that links the motor of the parasite to the cytoskeleton of the host cell and is presumed to be made up of rhopty neck proteins and apical membrane antigen 1(table 4).

During the last stage of merozoite development, several biological activities ensue to instigate invasion and expression of specific invasion ligands. From gene ontology functional enrichment data in this study, we predicted two key biological processes highly involved in invasion as gene expression and translation, as well as others with high percentage of occurrence (table 1). These biological processes are highly involved in protein production, which is the main result of gene expression, transcription and mRNA translation. These processes are coordinated just-in-time to fine-tune protein levels as required in invasion process, and also to evade immune function. Regulation of eukaryotic gene expression is complex, ranging from pre-transcriptional to post-translational regulation. The transcriptional level is believed to have the most stringent control of gene expression, although post-transcriptional mechanisms have surfaced as essential modulators.

The results of the functional enrichment and pathway enrichment analysis in table 1 and 2 suggest distinct biological mechanisms of gene expression, translation and post-transcriptional control of the investigated stages of P.f. lifecycle. Our results also revealed that ‘just-in-time’ transcriptional and translational schemes co-exist and manage proteins being expressed at the parasite development period.

V. CONCLUSIONS

Computational approaches which are faster and efficient than experimental approaches that happen to be time consuming and effort driven have been used to predict 1,510 protein-protein interactions that are likely to be implicated in the invasion of the RBCs by the malaria parasite. A number of these predictions are novel, while a good number are consistent with results from previous studies. The novel PPIs predicted can be experimentally investigated further for drug targets that can be of therapeutic interest.

SUPPLEMENTARY DOCUMENTS

The datasets used/or analyzed during this study are available with the first/corresponding author.

ACKNOWLEDGMENT

This work is partially supported by the Federal Polytechnic, Ilaro staff development programme and the NIH H3ABioNet grant U24HG006941.

REFERENCES

- [1] AF. Cowman, and BS. Crabb, “Invasion of the Red Blood Cells by Malaria Parasites”, *Cell*, Vol. 124, pp. 755-766, 2006.
- [2] AG. Maier, BM. Cooke, AF. Cowman, and L. Tilley, “Malaria parasite that remodel the host erythrocyte”, *PubMed*, vol. 7 no. 5, pp. 341-354, 2009.
- [3] MJ. Boyle, DW. Wilson, and JS. Richards, “Isolation of viable *Plasmodium falciparum* merozoites to define erythrocyte invasion events and advance vaccine and drug development” *P Natl Acad Sci*, vol. 107, pp. 14378-83, 2010.
- [4] A. Keeley, and D. Soldati, “The glideosome: a molecular machine powering motility and host-cell invasion by Apicomplexa” *Trends Cell Biol.*, Vol. 14, pp. 528-532, 2004..
- [5] N. Mohandas, and X. An, “Red blood cells and malaria” *IRON*, vol. 16, no. 35, pp. 454-467, 2009.
- [6] MJ. Boyle, DW. Wilson, and J.G Beeson, ”New approaches to studying Plasmodium falciparum merozoite invasion and insights into invasion biology” *Int J Parasitol*, vol. 43, pp. 1-10, 2013
- [7] P. Srinivasan, A. Yasgar, DK. Luci, W.L. Beatty, X. Hu, and J. Andersen, “Disrupting malaria parasite AMA1-RON2 interaction with a small molecule prevents erythrocyte invasion”, *Nat Commun.*, Vol. 4, no. 2261, 2013.
- [8] R. Chandramohanadas, BB. Russell, K. Liew, YH. Yau, and A Chong, “Small molecule targeting malaria merozoite surface protein-1 (MSP-1) prevents host invasion of divergent plasmodial species”, *J Infect Dis.*, Vol. 210, pp. 1616-26, 2014
- [9] DW. Wilson, CD. Goodman, BE. Sleebs, GE. Weiss, NWM. Jong, F. Angrisano, C. Langer, J. Baum, BS. Crabb, PR. Gilson, GI McFadden, and J.G. Beeson, “Macrolides rapidly inhibit red blood cell invasion by the human malaria”, *Plasmodium falciparum*. *BMC Biology* vol. 13, pp. 52. DOI: 10.1186/s12915-015-0162-0, 2015.
- [10] F. Teuscher, ML. Gatton, N. Chen J. Peters DE. Kyle, and Q. Cheng, “Artemisinin induced dormancy in plasmodium falciparum: duration, recovery rates, and implications in treatment failure”, *J Infect Dis.*, vol. 202, pp. 1362-1368, 2010.
- [11] KR. Hughes, GA. Biagini, and AG. Craig, “Continued cytoadherence of *Plasmodium falciparum* infected red blood cells after antimalarial treatment”, *Mol. Biochem Parasitol.*, vol. 169, pp. 71-8, 2010.
- [12] KI. Barnes, F. Little, A. Mabuza, N. Mgomezulu, J. Govere, and D. Durrheim, “Increased gametocytemia after treatment: an early parasitological indicator of emerging sulfadoxine-pyrimethamine resistance in falciparum malaria”, *J Infect Dis.*, vol. 197, pp.1605-1613, 2008
- [13] JG. Beeson, DR. Drew, MJ. Boyle, G. Feng, J.I. Fowkes, and J.S. Richards, “Merozoite surface proteins in red blood cell invasion, immunity and vaccines against malaria” *FEMS Microbiology Reviews*, vol. 40, no. 3, pp. 343-372, 2016.
- [14] TD. Otto, D. Wilinski, S. Assefa, TM. Keane, LR. Sarry, U. Böhme, and M. Berriman, “New insights into the blood-stage transcriptome of *Plasmodium falciparum* using RNA-Seq”, *Molecular microbiology*, vol. 76, no. 1, pp. 12-24, 2010.
- [15] MJ. Nueda, S. Tarazona, A. Conesa, “Next maSigPro: updating maSigPro bioconductor package for RNA-seq time series”, *Bioinformatics*, vol. 30, no. 18, pp. 2598-602, 2014.
- [16] DJ. LaCount, M. Vignali, R. Chettier, A. Phansalkar, R. Bell, J.R. Hesselberth, C. Kurschner, “A protein interaction network of the malaria parasite *Plasmodium falciparum*”, *Nature*, vol. 438, no. 7064, pp. 103-107, 2005.
- [16] AF. Cowman, and B.S. Crabb, “Invasion of the Red Blood Cells by Malaria Parasites”, *Cell*, Vol. 124, pp. 755-766, 2006.